

# Voxel Nodes Model Parameterization for GPS Water Vapor Tomography

Nan Ding, Shubi Zhang, Xin Liu and Yili Xia

**Abstract** Water vapor is the basic parameter to describe atmospheric conditions and the content of it in the atmosphere is rare for water circulation system, but it is the most active element with quick space-time change. GPS tomography is a powerful way to provide high spatiotemporal resolution of water vapor density. In general, water vapor tomography utilizes slant wet delay information from ground-based GPS network to reconstruct the humidity field. Space at the zenith directions of ground-based GPS is discretized into voxel both at horizontal and vertical direction; setting up tomographic equations by slant delay observations can work out vapor parameter in voxel. In this paper, spatial structure model of humidity field is constructed by voxel nodes, and new parameterizations for acquiring data of water vapor in the troposphere by GPS are proposed based on inverse distance weighted (IDW) interpolation in horizontal and vertical interpolation function in vertical. Unlike the water vapor density is constant within a voxel; the density at a certain point is determined by new parameterizations. This algorithm avoids using horizontal constraint to smooth some voxels that not be crossed by satellite rays. Grouping and sorting access order scheme is introduced to minimize correlation between SWV observations. Three experimental schemes for GPS tomography are carried out using 7 days of Hong Kong Satellite Positioning Reference Station Network (SatRef). The results indicate that water vapor density derived from 4 nodes parameterization are most robust than 8 nodes and 12 nodes.

**Keywords** GPS water vapor tomography · Inverse distance weighted interpolation · Vertical interpolation function · Grouping and sorting access order

---

N. Ding (✉) · S. Zhang · X. Liu · Y. Xia  
School of Environment Science & Spatial Informatics, CUMT,  
1 Daxue Road, Xuzhou, China  
e-mail: metdingnan@163.com

© Springer Nature Singapore Pte Ltd. 2017  
J. Sun et al. (eds.), *China Satellite Navigation Conference (CSNC) 2017  
Proceedings: Volume I*, Lecture Notes in Electrical Engineering 437,  
DOI 10.1007/978-981-10-4588-2\_20

233

## 1 Introduction

Based on the GPS meteorology technique [2], two experiments promoted the development of GPS integrated water vapor (IWV) inversion: GPS/STORM [13] and the GPS–Winter Icing and Storms Project experiment [6]. Both experiments showed that GPS is a cost-effective and reliable means of continuously monitoring IWV with accuracies comparable to water vapor radiometer (WVR) and radiosonde (RS). However, the IWV is a measure of the total amount of water vapor above a certain station and it cannot provide the information on the spatial distribution of water vapor. In order to meet the demand, GNSS water vapor tomography [1, 3–5, 7, 10, 14–16, 19] came out as a promising method providing information on the four-dimensional distribution of the water vapor in the troposphere.

In this paper, a new parameterized approach instead of traditional constraints is introduced, which is based on IDW interpolation and vertical interpolation function. The new algorithm is investigated by the data of SatRef. The experiment mainly analyzes and discusses the influences of different numbers of voxel nodes on the results of GPS water vapor tomography. The question about some voxels may not be crossed by any signals is addressed by IDW interpolation.

## 2 Voxel Nodes Model Parameterization for GPS Tomography

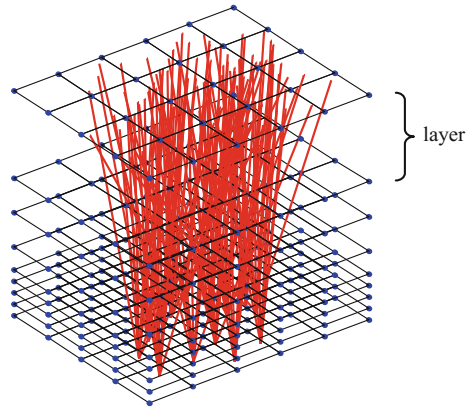
The slant water vapor (SWV) is the integrated water vapor along the slant path. Specific GPS processing techniques provide this product as the observations for GPS tomography. Using SWV input data the tomography observations in the absolute humidity can be expressed by [1]:

$$SWV = \int_s H_s ds + RB \quad (1)$$

where  $H_s$  is the absolute humidity,  $s$  is the slant path,  $RB$  is the partial water vapor caused by ray bending. The second term is due to ray bending. However, the effect of this geometric water vapor, making much smaller contribution to SWV, can be neglected [8].

Voxel nodes model (VNM) parameterization assumes that troposphere is divided into a numbers of layers which constructed by neighboring parallel planes (see Fig. 1). The voxel nodes (blue points) are designed in each plane. SWV produced by one signal (red line) is discretely modeled by the value at points of intersection between straight line and planes.

**Fig. 1** Voxel nodes structure of GPS tomography model and the distribution of signal rays (red line) crossing the layers, the value of SWV divides into the value of water vapor at voxel nodes (blue point)



In the VNM parameterization, Eq. 1 is decomposed into sum of piecewise integration:

$$SWV = \sum_{i=1}^n \int_{s_i}^{s_{i+1}} H_s(i) ds \tag{2}$$

where n is the number of layer, Hs(i) is the absolute humidity in i-th of layer.

Piecewise integration in Eq. 2 can be addressed through Newton-Cotes formulae [11]. It is assumed that the value of piecewise integration defined on  $[s_i, s_{i+1}]$  is known at equally spaced point  $p_1$ - $p_5$  (see Fig. 2). This allows the integral in Eq. 2 to be expressed as a weighted sum of the water vapor density at the voxel nodes. In this paper, the closed Newton-Cotes formula of degree 4 is utilized with water vapor density at the 5 equally spaced points. Point  $p_1$  and  $p_5$  in the plane  $i$  and  $(i + 1)$  respectively can be estimated by inverse distance weighted (IDW) interpolation. IDW parametrical method explicitly implements the assumption that the value of water vapor density that are close to one another are more alike than those that are farther away. The IDW interpolation can be given as

$$P_{IDW} = \begin{cases} \frac{\sum_{j=1}^m D(P, x_{node}^j)^{-1} \cdot x_{node}^j}{\sum_{j=1}^m D(P, x_{node}^j)^{-1}}, & \text{if } D(P, x_{node}^j) \neq 0 \text{ for all } j \\ x_{node}^j, & \text{if } D(P, x_{node}^j) = 0 \text{ for some } j \end{cases} \tag{3}$$

where  $D(P, x_{node}^j)$  is the distance between pierce point  $P_{IDW}$  and voxel node  $x_{node}^j$ ,  $x_{node}^j$  is the value of water vapor at a certain voxel node, and m is the number of voxel node which is used for IDW interpolation. In the case of point  $p_2$ - $p_4$ , correspondence between the value of equally spaced points and projection points would be defined by using vertical interpolation function (VIF) in the relatively

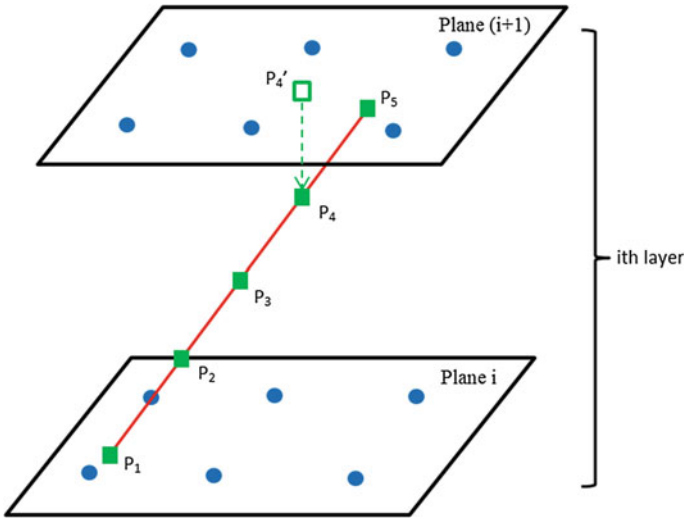


**Fig. 2** Voxel nodes parameterized design based on the closed Newton–Cotes formula of degree 4 and interpolation. Voxel nodes (blue points) are used for equally spaced points (green square) interpolation.  $P'_4$  (green hollow square) is projection point of  $P_4$  in plane (i + 1)

nearby plane between plane i and (i + 1). VIF based on the exponential law [12, 17] can be expressed by the formula

$$P = P'_{IDW}e^{-Z/H} \tag{4}$$

where  $P$  is the water vapor density of the equally spaced points,  $P'_{IDW}$  is the water vapor density of projection points which can be expressed by Eq. (3),  $Z$  is the height between  $P$  and  $P'_{IDW}$ ,  $H$  is the water vapor scale height, which can be calculated by Eq. (5) [18]

$$H = \frac{10W}{\rho_s} \tag{5}$$

where  $W$  is the vertical total water vapor content in  $g/m^2$ ,  $\rho_s$  is the surface humidity in  $g/m^3$ .  $W$  can be obtained from PWV. Ground-based GPS network, for the purpose of meteorological monitoring, provides meteorological parameter, which can be used for calculating  $\rho_s$ .

However, grid points not used in any interpolation should not generally be avoided. In fact, this case often occurs in lower-level layers with the 4 nodes method, and occurs less often when many points are included in the interpolation. We also address “empty” grids using the inverse distance weighted (IDW) interpolation. The values of an “empty” grid are estimated by the “non-null” grids around it.

Based on Eqs. (2)–(4), the GPS tomography equations could be constructed

$$A \cdot X = b \quad (6)$$

where  $A$  is the coefficient matrix of GPS tomography model,  $b$  presents the SWV observations vector,  $X$  is the value of the humidity at all designing voxel nodes.

Algebraic reconstruction techniques (ART) have successfully been used to reconstruct the humidity field [1, 3]. An advantage of ART is that it has high numerical stability even under bad conditions and it is relatively easy to incorporate prior knowledge into the reconstruction process.

In our study, grouping and sorting access order [9] is used for improving the accuracy of inversion. It is desirable to order the SWV observations (SWVs) such that subsequently applied SWV are largely uncorrelated. This means that consecutively available SWVs must have significantly different values, because the value of SWV is determined by the azimuth and elevation angles of a signal. If the SWV in a set have similar values solved by ART, the results tend to move away from the desired solution, which delays convergence. To summarize, the principle of SWV access order is that in a subsequence of iterations, steps should be as independent as possible from the previous steps.

### 3 GPS Tomography Results

#### 3.1 Tomography Strategy

SatRef is a local satellite positioning system covering the extent of Hong Kong. The network consists of 18 Continuously Operating Reference Stations (CORS) and 14 of them were used in this study. The area of investigation ranges from  $113.749^\circ$  to  $114.474^\circ$ E longitude and from  $22.115^\circ$  to  $22.651^\circ$ N latitude (Fig. 3a) with a height domain of 0–10,800 m (Fig. 3b). The horizontal and vertical station distributions are presented in Fig. 3a and Fig. 3b, respectively. The number of spatial voxel nodes (Fig. 3a) using for tomography are  $6 \times 4 \times 10$  with a horizontal resolution of 0.145 (15 km). Non-uniform layers are adopted with the interval from 500 to 3800 m (Fig. 3b). We made the hypothesis that all the value of water vapor at any point in the plane is determined by a weighted average of the value at voxel nodes that closest the point. The experiments used for reconstruction of the humidity field covered a seven-day period from August 9–15, 2015 (day of year, DOY 221–227). Samples of GPS and surface meteorological data are obtained in 30 s intervals, with a temporal resolution of 30 min.

The data from Hong Kong network are processed with GAMIT software version 10.5. Based on number of voxel nodes are used for IDW interpolation points  $P$ , three sets of schemes are presented

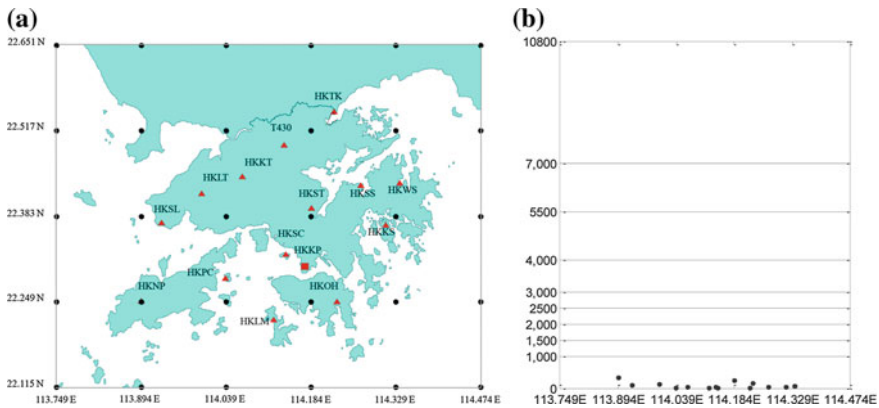


**Fig. 3** **a** Distribution of the Hong Kong reference stations (red triangle) and the King's Park meteorological station (red square). The gray wireframe indicates the plane that contains voxel nodes (black dot) using in the tomographic processing. The study area was discretized into  $6 \times 4 \times 10$  voxel nodes for the water vapor tomography. **b** The vertical structures of the voxel nodes model used in the tomographic processing

- 4 nodes: four voxel nodes (neighbors) from voxel nodes model will be used
- when calculating a water vapor value for the piercing point.
- 8 nodes: eight voxel nodes will be used when calculating a water vapor value for the piercing point.
- 12 nodes: twelve voxel nodes will be used when calculating a water vapor value for the piercing point.

### 3.2 Analysis of Total Statistics

Three kinds of solutions compare with radiosonde data (RS) in Hong Kong. Because of limited space, only a representative example at 2015–08–09 (DOY 221) UTC 0 and 12 is shown (see Fig. 4). It is clear that all of the water vapor profiles increasing height. At UTC 12, the variation of water vapor from radiosonde data presents disturbance instead of keeping smooth decrease. But the tomographic solutions keep consistent with changing trends of radiosonde data. In each plane (Fig. 3b), mean water vapor density in voxel nodes are computed. It indicates that the humidity with high spatial resolution (e.g. radiosonde) is difficult to retrieve because of the limited accuracy of tomography solution. It is difficult to judge which scheme is best suited for GPS water vapor tomography from the statistics of RMSE, IQR and BIAS data (Table 1). These methods have their advantages respectively; 4 nodes parametrization presents more accurate results than others from RMSE. The inter quartile range (IQR), to some extent, reflects the discreteness of datasets. Based on the value of IQR (Table 1) and scatter plots of water

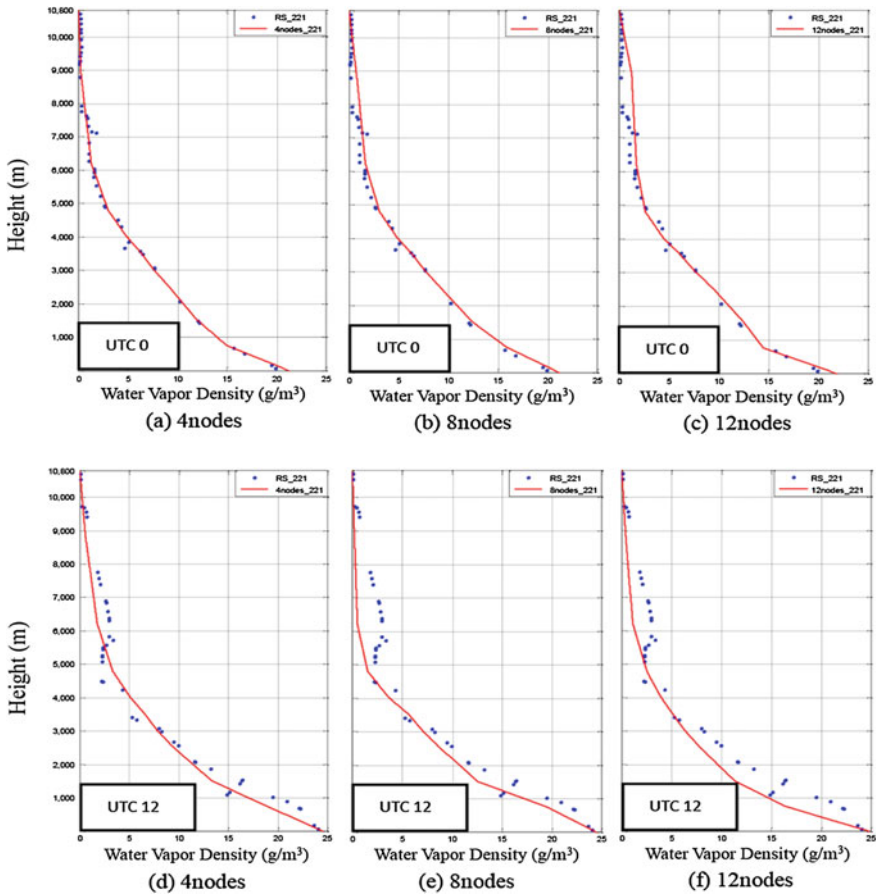


**Fig. 4** Comparison of HKKP’s radiosonde data (blue dot) with three sets of water vapor tomography schemes (red lines) at DOY 221 2015 UTC 0 and 12, respectively. (red lines) reconstructed by tomographic solutions accord with radiosonde data. At UTC 0, all profiles and the scatter of radiosonde data decrease exponentially with increasing height. However, at UTC 12, radiosonde data unable to keep smooth

vapor density (Fig. 5), it is clear to find that tomographic solutions computed by 4 nods and 8 nodes parameterizations more concentrated than 12 nodes.

However, compared with the first two methods, 12 nodes tomographic has a smallest negative bias (Table 1) with highest discretization. These statistical properties of the differences between three parametrizations and radiosonde data are also presented by box plots (Fig. 5d). It contains five characteristic values: the first and third quartiles (Q1 and Q3) at the bottom and top of the box, the second quartile (Q2) is located inside the box (the median) and the ends of the whiskers (upper and lower bound) at  $Q1 - 1.5(IQR)$  and  $Q3 + 1.5(IQR)$ . In addition, whiskers are applied to detect outliers (cross in Fig. 5d). All of these are summarized in Table 1.

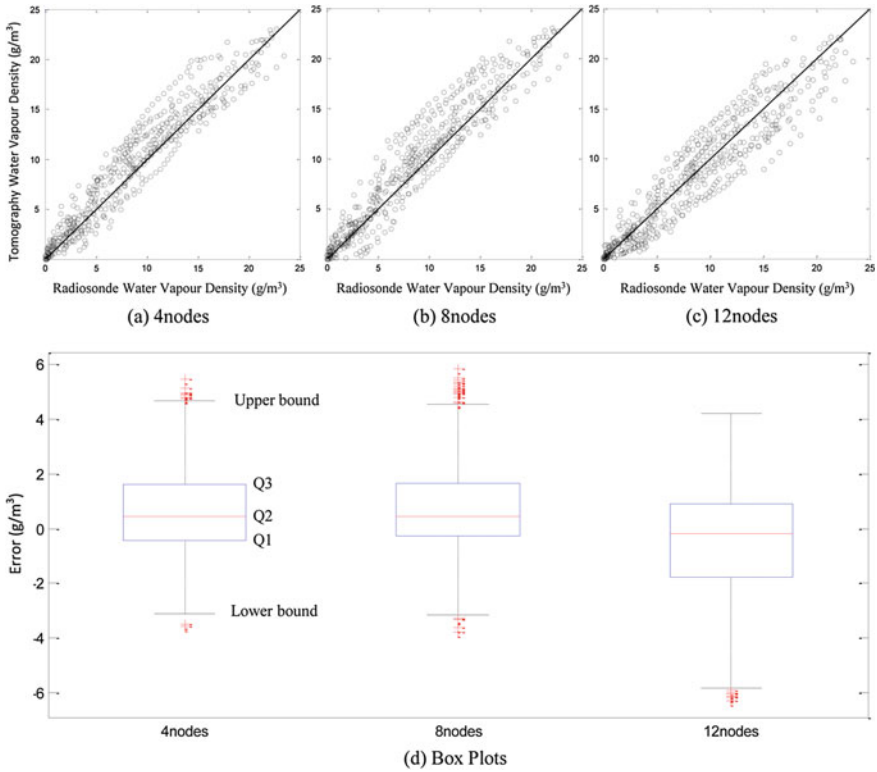


**Fig. 5** Tomographic solutions compared with radiosonde data. **a–c** Scatter plots of water vapor density with 4 nodes, 8 nodes and 12 nodes parameterization and **d** Box plots of the difference between three parameterization methods and radiosonde data at UTC0 and UTC12 from August 9 to 15, 2015

**Table 1** Statistics between three parameterizations and water vapor measurements constructed by HKKP’s radiosonde data for 7 days (DOY 221–227) in 2015

Statistics	4 nodes	8 nodes	12 nodes
RMSE (g/m <sup>3</sup> )	1.857	2.016	2.092
IQR (g/m <sup>3</sup> )	1.948	2.048	2.702
BIAS (g/m <sup>3</sup> )	0.65	0.742	-0.336
Q1	-0.42	-0.275	-1.792
Q2	0.436	0.458	-0.169
Q3	1.628	1.673	0.91
Upper bound	4.701	4.594	4.964
Lower bound	-3.4925	-3.196	-5.846
Number of outliers	16	34	8



IQR is the difference between Q3 and Q1 quartiles. It is important because IQR represents the spread of data and unlike total range, it is not affected by outliers. Q2 is the measure of central tendency and in good accordance with the bias. Upper and lower bound can be used to identify outliers. The 12 nodes has the smallest number of outliers, but it also has maximum bounds. 4 nodes and 8 nodes have similar bounds. However, if we use the bounds of 4 nodes, the number of outliers is 34 and 58 in 8 nodes and 12 nodes respectively. So compare 4 nodes parametrization with others has relative minimal outliers

## 4 Conclusion and Outlook

In this paper, a new GPS tomographic parameterization approach is proposed in our study. This approach can reconstruct a humidity field without using horizontal constraint and avoid some voxels not be crossed by satellite rays. On the other side, instead of dividing the troposphere into several layers with identical height, the vertical structure of tomography model adopts non-uniform layers to satisfy inherent characteristics of water vapor distribution and to lower the effect of difference magnitude between the calculated tomographic results. In order to minimize correlation in projection access, grouping and sorting access order scheme is developed to order the SWV observations in such a way that subsequently applied values of SWVs are largely uncorrelated. Based on number of voxel nodes is selected for IDW interpolation, three schemes are designed to retrieve water vapor density in voxel node.

Results of Hong Kong tomographic experiments using GPS data from DOY 221–227, 2015 show that this proposed approach is validated for GPS tomography. We discuss and analyze 4 nodes, 8 nodes and 12 nodes parameterizations. The 4 nodes method has highest accuracy with perturbations of  $1.857 \text{ g/m}^3$  compare to the two other methods regarding the overall dataset. However, due to the limitation of tomographic accuracy, mean water vapor density computed by GPS tomography is hard to retrieve humidity field with the high spatial resolution of radiosonde. From results of different statistical methods, we can draw a conclusion that 4 nodes parametrization has relative minimal outliers and the error caused by it more concentrated than others. It means that tomographic results derived from 4 nodes have a higher stability and reliability.

Further investigations are needed to improve the horizontal structure of humidity field by adjust node position in each layer to fit distribution of satellite rays. Flexible layout is the advantage of voxel nodes model. In the future, fusion of GNSS and external measurements from other sensors in GPS tomography system will be a prospective direction to enhance stability and reliability of water vapor tomography and to decrease intervals of tomography.

## References

1. Bender M, Dick G, Ge M et al (2011) Development of a GNSS water vapor tomography system using algebraic reconstruction techniques. *Adv Space Res* 47:1704–1720
2. Bevis M, Businger S, Herring TA et al (1992) GPS meteorology: remote sensing of atmospheric water vapor using the global positioning system. *J Geophys Res Atmos* 97:15787–15801
3. Chen B, Liu Z (2014) Voxel-optimized regional water vapor tomography and comparison with radiosonde and numerical weather model. *J Geodesy* 88:691–703
4. Flores A, Ruffini G, Rius A (2000) 4D tropospheric tomography using GPS slant wet delays. *Ann Geophys-Ger* 18:223–234
5. Gradinarsky LP, Jarlemark P (2004) Ground-based GPS tomography of water vapor: analysis of simulated and real data. *J Meteorol Soc Jpn* 82:551–560
6. Gutman S, Chadwick R, Wolfe D et al. (1995) Toward an operational water vapor remote sensing system using the global positioning system. Environmental Sciences Div, USDOE Office of Energy Research, Washington, DC (United States)
7. Hirahara K (2000) Local GPS tropospheric tomography. *Earth Planets Space* 52:935–939
8. Ichikawa R, Kasahara M, Mannoji N et al (1995) Estimations of atmospheric excess path delay based on three-dimensional, numerical prediction model data. *J Geodetic Soc Jpn* 41:379–408
9. Nan D, Shubi Z (2016) Land-based GPS water vapor tomography with projection plane algorithm. *Acta Geod et Cartographica Sin* 45:895–903
10. Nilsson T, Gradinarsky L (2006) Water vapor tomography using GPS phase observations: simulation results. *IEEE T Geosci Remote* 44:2927–2941
11. Perler D, Geiger A, Hurter F (2011) 4D GPS water vapor tomography: new parameterized approaches. *J Geodesy* 85:539–550
12. Reitan CH (1963) Surface dew point and water vapor aloft. *J Appl Meteorology* 2:776–779
13. Rocken C, Hove TV, Johnson J, Solheim F, Ware R, Bevis M, Chiswell S, Businger, S (1995) GPS/STORM-GPS sensing of atmospheric water vapor for meteorology. *J Atmos Ocean Tech* 12:468–478
14. Rohm W (2013) The ground GNSS tomography-unconstrained approach. *Adv Space Res* 51:501–513
15. Seko H, Shimada S, Nakamura H et al (2000) Three-dimensional distribution of water vapor estimated from tropospheric delay of GPS data in a mesoscale precipitation system of the Baiu front. *Earth Planets Space* 52:927–933
16. Song SL, Zhu WY, Ding JC et al (2006) 3D water-vapor tomography with Shanghai GPS network to improve forecasted moisture field. *Chin Sci Bull* 51:607–614
17. Tomasi C (1981) Determination of the total precipitable water by varying the intercept in reitan's relationship. *J Appl Meteorology* 20:1058–1069
18. Tomasi C (1977) Precipitable water vapor in atmospheres characterized by temperature inversions. *J Appl Meteorol* 16:237–243
19. Yao YB, Zhao QZ, Zhang B (2016) A method to improve the utilization of GNSS observation for water vapor tomography. *Ann Geophys-Ger* 34:143–152